

Supplemental Figure 1

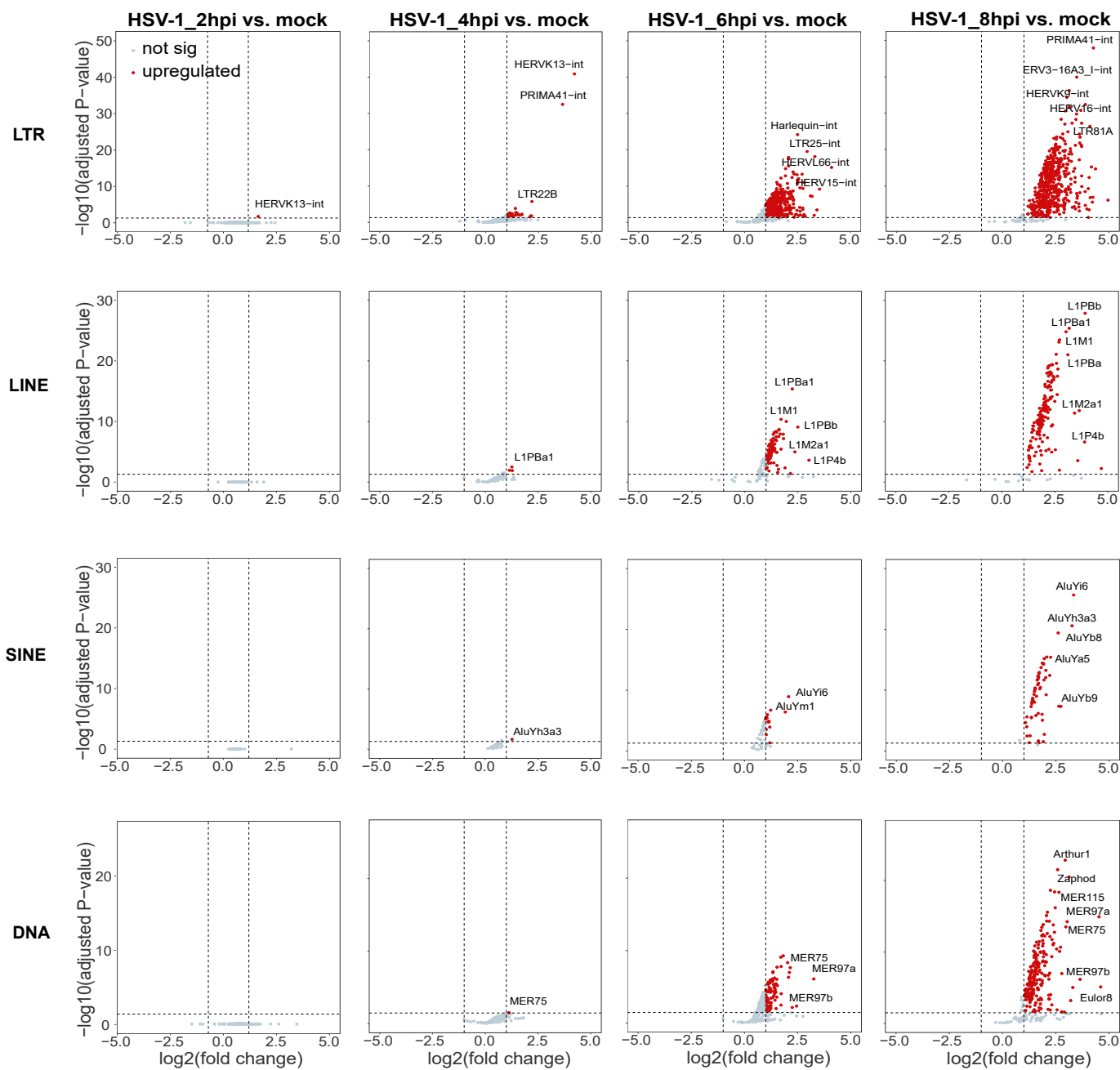


Fig.S1 Volcano plot showing significantly upregulated TEs of 4 subclasses (LTR, LINE, SINE and DNA respectively) upon HSV-1 infection at 2, 4, 6, and 8 hpi in HFF cells. Red dots indicate TEs meeting the criteria of $\log_2(\text{FC}) > 1$ and $P < 0.05$.

Supplemental Figure 2

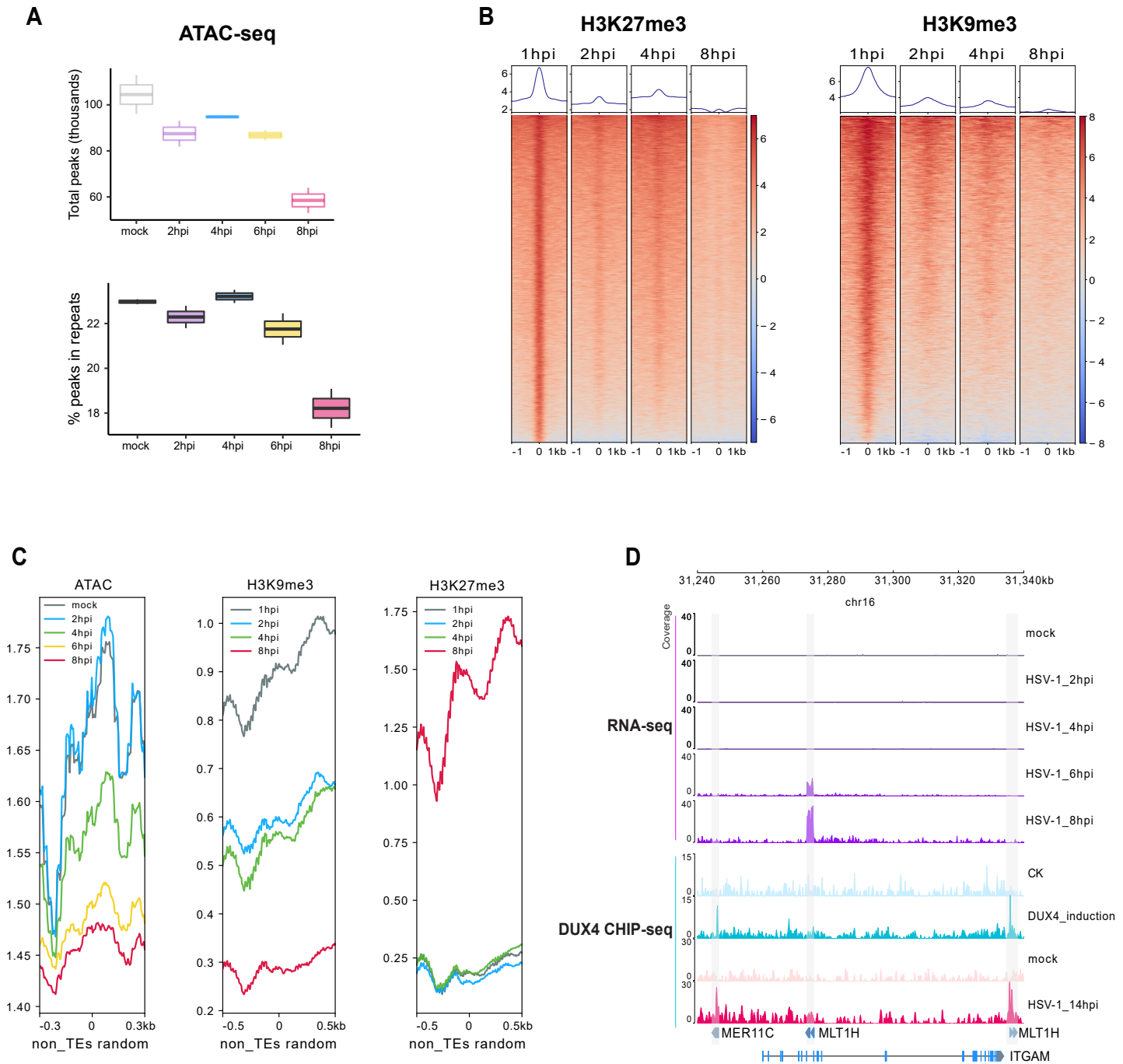


Fig.S2 (A) Number of peak regions detected in ATAC-seq. of both mock and HSV-1-infected HFF cells (upper panel) and proportion of ATAC-seq peaks that overlap with repeat regions (lower panel). **(B)** Heatmap displaying enrichment levels of TEs with downregulated H3K9me3 and H3K27me3 markers upon HSV-1 infection at 1, 2, 4 and 8 hours post-infection (hpi) in HFF cells. **(C)** Peak count frequency of ATAC-seq as well as CHIP-seq peaks of transcriptional repression marks (H3K9me3 and H3K27me3) overlapping with 100000 random non-TEs region. **(D)** Schematic representation and RNA-seq tracks illustrate the expression dynamics of the TEs MLT1H and the gene ITGAM during HSV-1 infection at mock, 2, 4, 6, and 8 hpi. Schematic representation and CHIP-seq tracks illustrate the binding of DUX4 to the TEs MER11C and MLT1H after DUX4 induction and HSV-1

Supplemental Figure 3

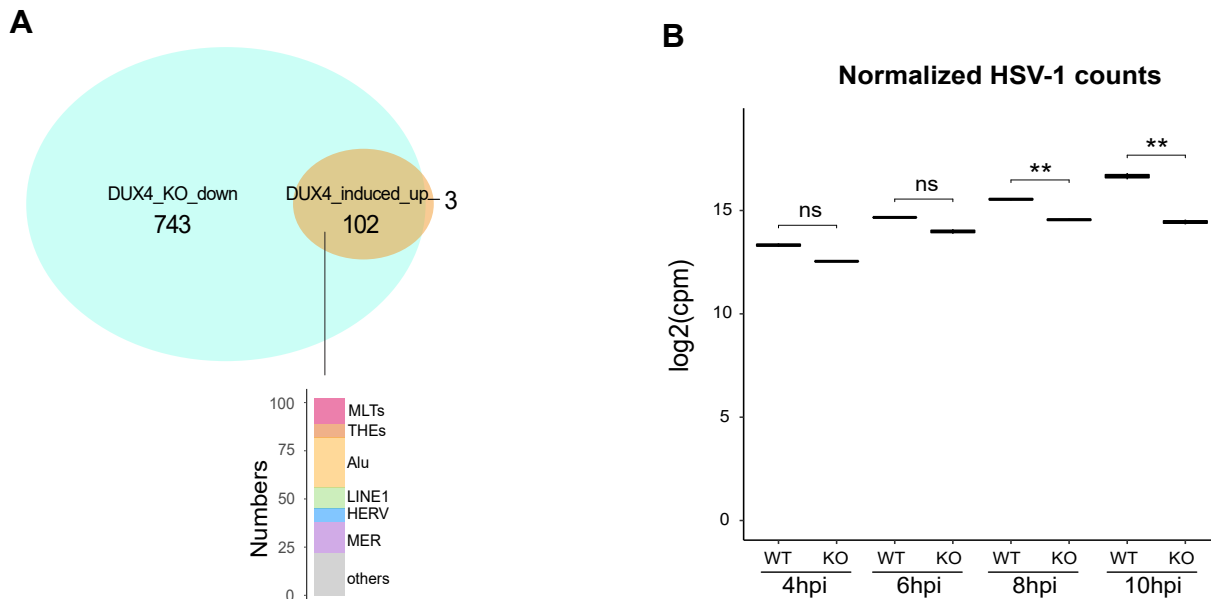


Fig.S3 (A) Venn diagram showing the overlap of activated TEs in DUX4-induced 293T cells and TEs down-regulated in DUX4 KO cells upon HSV-1 infection at 8hpi. **(B)** Box plot showing the normalized HSV-1 counts of DUX4 KO and WT HAP1 cells upon HSV-1 infection at 4, 6, 8 and 10 hpi. Statistical significance was determined using t-test (ns: not significant, **P < 0.01).

Supplemental Figure 4

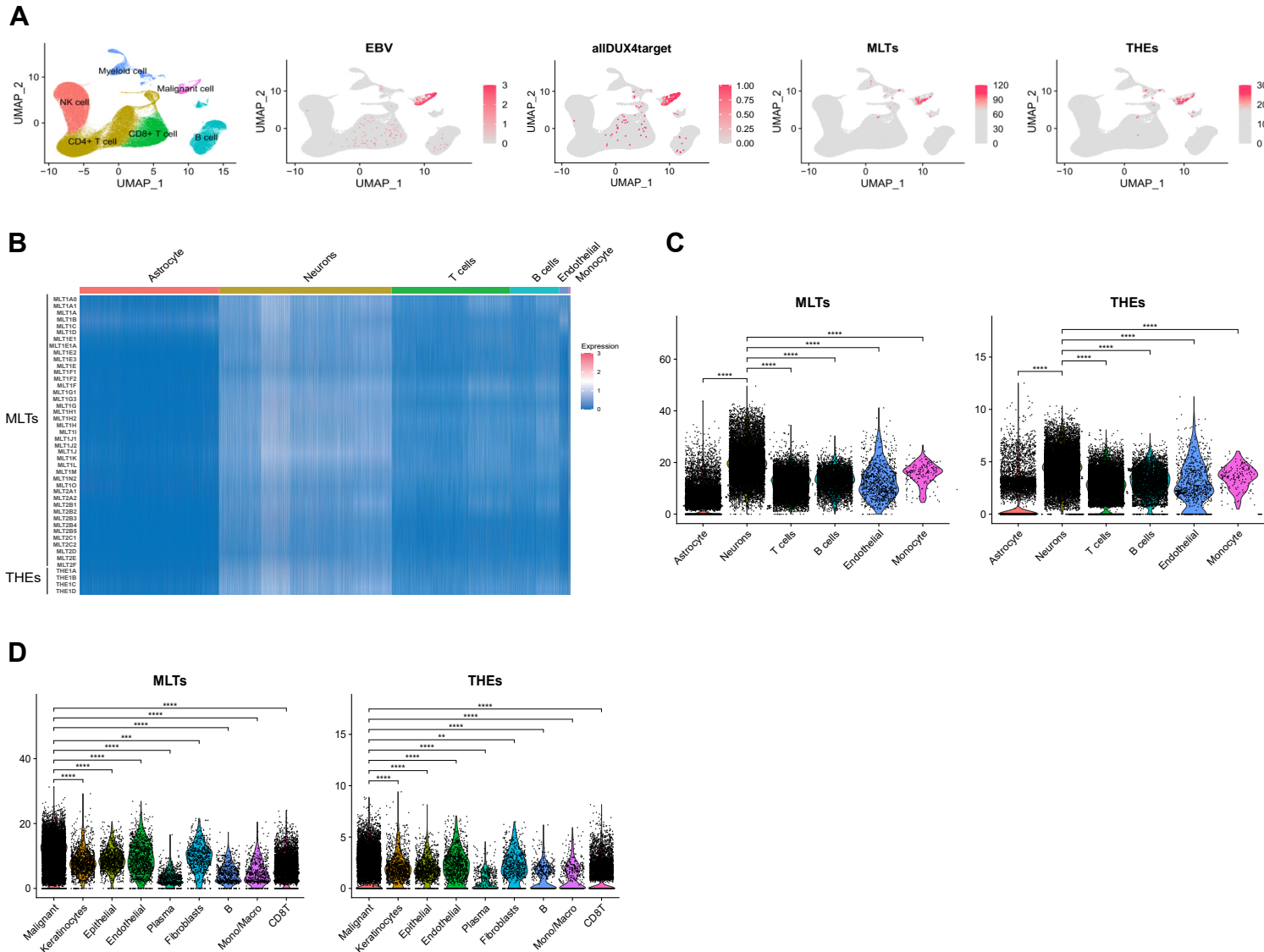


Fig.S4 (A) Nasopharyngeal Carcinoma Patients with Epstein-Barr Virus (EBV) Positive: First panel: Cell identity map. Second panel: UMAP projection of normalized EBV-specific reads per cell. Third panel: UMAP projection of normalized DUX4-target reads per cell. Fourth panel: normalized MLTs reads per cell. Fifth panel: UMAP projection of normalized THEs reads per cell. **(B)** Heatmap illustrates the normalized reads number of MLTs and THEs members across all cell types in Merkel Cell Carcinoma (MCC) tumor patients with Merkel Cell Polyomavirus (MCV) Positive. **(C)** Merkel Cell Carcinoma (MCC) tumor patients with Polyomavirus (MCV) Positive: A series of violin plots that highlight the distribution of the normalized MLTs reads per cell and normalized THEs reads per cell in different cell types respectively. Statistical significance was determined using two-sided nonparametric Wilcoxon rank-sum tests (* $P < 0.05$, ** $P < 0.01$, *** $P < 0.001$, **** $P < 0.0001$). **(D)** Head and Neck Squamous Cell Carcinoma (HNSCC) Patients with Human Papillomavirus (HPV) Positive: A series of violin plots that highlight the distribution of the normalized MLTs reads per cell and normalized THEs reads per cell in different cell types respectively. Statistical significance was determined using two-sided nonparametric Wilcoxon rank-sum tests (* $P < 0.05$, ** $P < 0.01$, *** $P < 0.001$, **** $P < 0.0001$).

Supplemental Figure 5

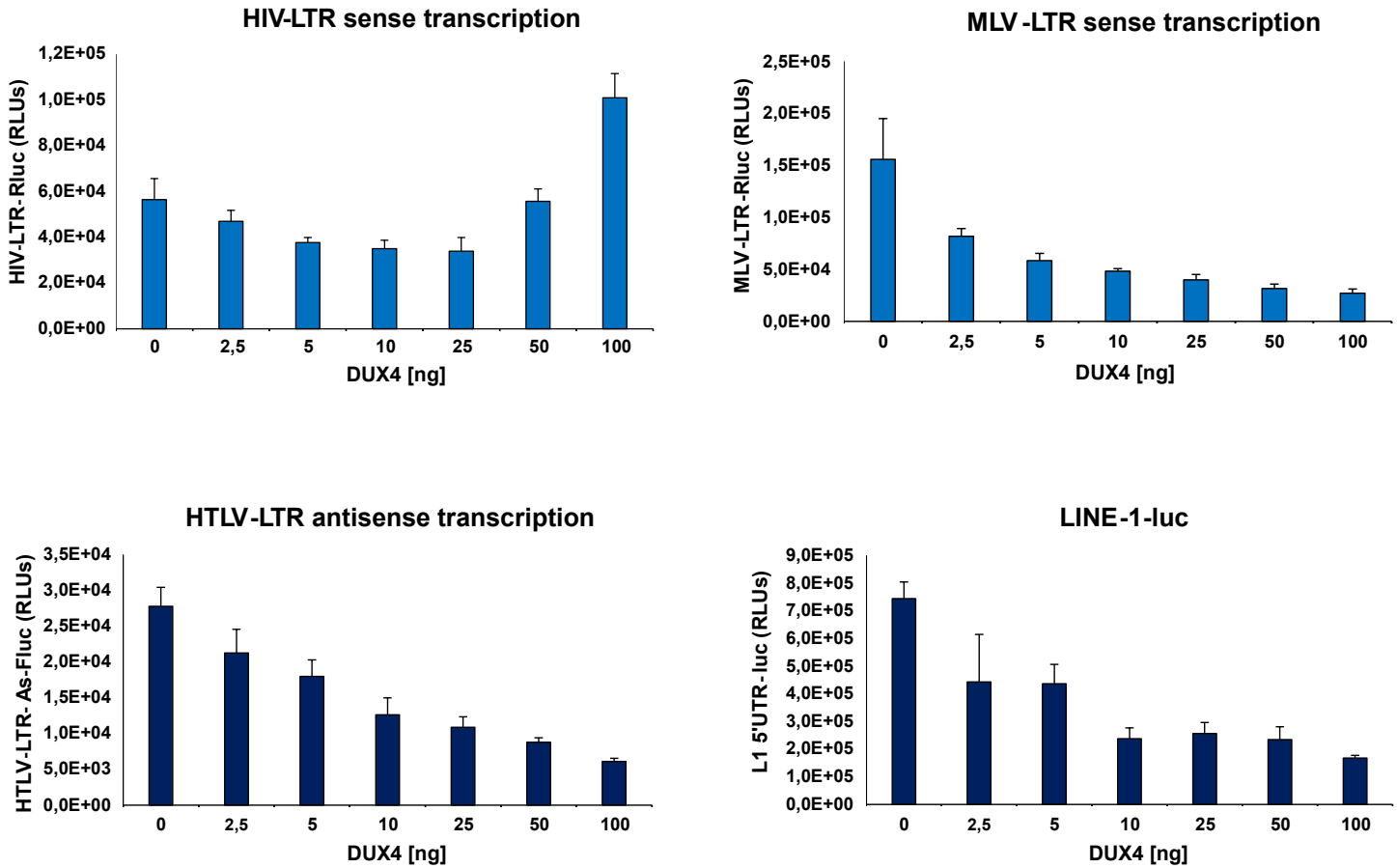


Fig.S5 DUX4 affects HIV-LTR, MLV-LTR, HTLV-LTR and LINE-1 transcription. The graphs show the average RLU values of Luciferase assays of LTR-Luciferase constructs in the presence and absence of DUX4 of one representative of n=3 experiments. Error bars represent the standard deviation of the mean.